

BUILDING MODELING BY THE INTEGRATION OF MULTI-SOURCE DATA

Liang-Chien Chen¹, Tang-Yu Li², Tee-Ann Teo³

¹Professor, ²Msc Student, ³PhD Candidate

Center for Space and Remote Sensing Research,

National Central University, Taiwan

E-mail: lcchen@csrsr.ncu.edu.tw; 943202068@cc.ncu.edu.tw; ann@csrsr.ncu.edu.tw

KEY WORDS: Building Model, LIDAR Data, Aerial Images, 2-D map, Reconstruction.

ABSTRACT: Due to the complexity and variety of the building types, using single data to automatically generate building models could yield unreliable results. Therefore the trend is to fuse multi-source data to achieve the automation. This research, thus, considers the integration of LIDAR data, aerial images, and 2-D maps to perform the modeling. The proposed scheme comprises three major steps: (1) data preprocessing, (2) classification of roof types, and (3) building modeling. In the first step, we enclose the polylines of the maps then extract the point clouds that belong to a building. Through the roof hypothesis by employing point clouds, the camber roofs are parameterized. For non-camber roofs, we determine the ridges of gable roofs by interesting the two inclined planes. The step-edges are obtained by combining point clouds and image features. Finally, we shape the models by SMS method. The result of classification shows that different kinds of roofs can be correctly categorized. Buildings are successfully reconstructed by the proposed approach.

1. INTRODUCTION

In response to the development of 3-D city spatial information for urban planning and management, the establishment of cyber city is getting important. Cyber city is an epitome of the real world. It stores and reconstructs the information of real world in the system. The information provides valuable decision support to city managers. The applications of the cyber city are significant, such as urban planning (Mannan and Juergen, 2004), environmental planning, change detection (Habib et al., 2005), and disaster risk management, etc.

Building models is one of the most important parts in a cyber city. Building reconstruction could be accomplished by two strategies, i.e., fully automatic approach and semi-automatic approach. Fully automation is always an ultimate goal in building reconstruction. However, it is difficult to achieve fully automatic interpretation. Thus, many application projects adopt semi-automatic method in the model production.

Building models may be reconstructed by different approaches such as using aerial photography which picks up the model and modulates the parameters by manual operation then shaping by CSG method (Tseng and Wang, 2003). It might also be restricted to the simple shape by polyhedral models (Taillandier, 2005). Some combined aerial images with maps to locate the working area and generate building hypotheses then fitting by CSG models (Suveg and Vosselman, 2004). Since LIDAR (light detecting and ranging) has plentiful 3-D information, it has demonstrated profound potentials in automatic building reconstruction. In the past researches, many reports used LIDAR data to reconstruct building models such as projecting point clouds in 2-D space to analyze the 3-D plane (Schwalbe et al., 2005). Some integrate cadastral data to analyze the relation between 3-D planes then reconstruct by B-rep model

(Overby et al., 2004). Some combined LIDAR with map and images, generate the initial model then reconstruct model by bundle adjustment (Zhang et al., 2005).

The generation of building models, in general, includes two major steps: detection and reconstruction. Since the 2-D maps provide the boundaries of buildings, the focus of this research is the reconstruction part. Considering the varieties of building, this investigation handles flat, gable, and camber roofs by incorporating vector maps, aerial images and LIDAR point clouds. Since the camber and gable roofs have weak features in the image space, LIDAR data provides complementary 3-D information in the reconstruction. On the other hand, if the density of the LIDAR point clouds is not sufficient for the reconstruction, we integrate the image features into the scheme. The workflow of investigation is shown in Fig. 1.

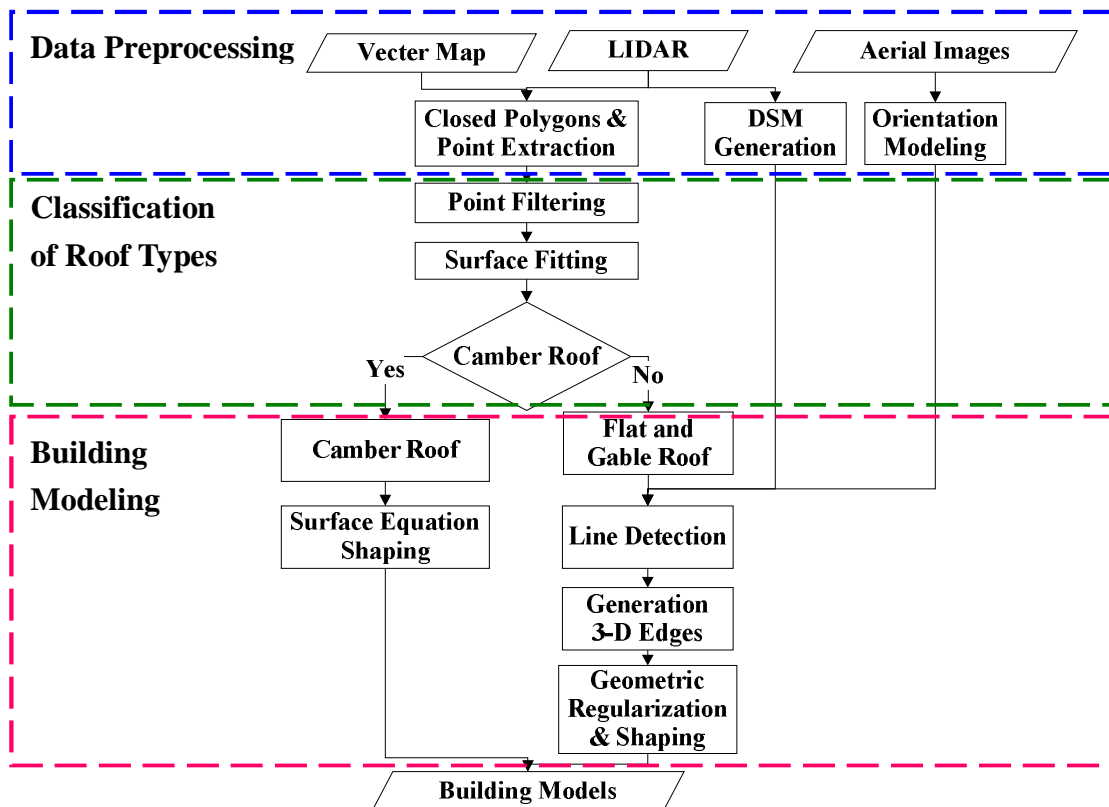


Figure 1 Workflow of the proposed scheme

2. DATA PREPROCESSING

The preprocessing includes four parts. The first one is to establish the topology of the building boundaries. Since the vector data for buildings that we will use is the polyline representation, no topology is built. Thus, we use SMS method (Rau and Chen, 2003) to rebuild the topology. The boundaries are, thus, enclosed. The second part is to select those point clouds that belong to the buildings. The point-in-polygon technique (Mortenson, 1999) is taken to select points inside the building polygons. The third part in the preprocessing is to calculate the orientation parameters for the aerial images. Some ground control points are measured to perform the modeling for orientation. It is done in such a way that the point clouds, vector maps, and images are co-registered in a unified coordinate system. The fourth part is to generate a grid DSM (digital surface model) from the LIDAR point clouds. The model will be used to locate the approximate position for the back projection in the generation of 3-D edges.

3. CLASSIFICATION OF ROOF TYPES

Prior to the building shaping, we categorize the roof types by using the point clouds. Once the most likely roof type of a building is determined, the surface function can be assured by fitting the point clouds. To better represent the surface, the point clouds need to be filtered.

3.1 Point Cloud Filtering

Considering the possible registration errors between LIDAR data and vector maps, the point clouds in a building polygon would include roof and ground points. A less number of points may also come from building walls. To obtain the points that solely belong to the roofs, we design a three-step processing for the filtering of unwanted points. In the first step, a clustering technique is employed to exclude non-roof points. Notice that the roof points should be the majority. In the next step, we eliminate the points that are deviated from the distribution with two standard deviations. That means we consider 95% confidence interval. Finally, the points that form over-steep facets are excluded. This step is dedicated to the exclusion of wall points. In the processing, TIN (triangulated irregular networks) structure is employed.

3.2 Surface Fitting

The shaping of the roofs deals with the determination of surface function for each roof primitive. We consider three types of the roofs in this investigation, namely, camber, flat, and gable. The roof structures are determined by the test of the most likelihood of the surfaces. For the camber roofs that have been assured by employing a sphere or a cylinder equation, the model may be reconstructed by the feature parameters. For those that do not belong to the camber roofs will be tested for the flat or gable roofs. To better delineate the roof details, each building area are split by the consideration of shape symmetry. A rectangle, for instance, in the Fig. 2 (a) is divided by two parts according to the first and second axes. Thus, the two possibilities in Fig. 2 (b) and Fig. 2 (c) are tested for the selection of the most likely one. In the determination, each part of A, B, C, and D is fitted with a plane. The one with the least fitting error are considered as the suitable roof.

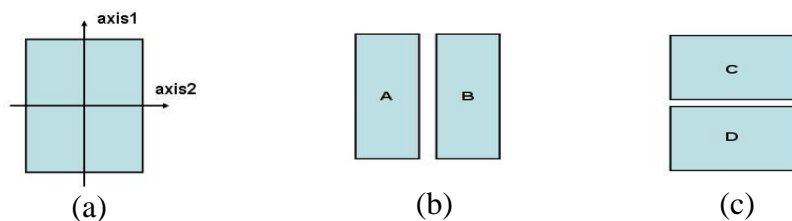


Figure 2 Splitting the building boundary
(a) Original roof polygon, (b) Divided by axis1, (c) Divided by axis2

4. BUILDING MODELING

Polyhedral models or parameter ones are considered in this investigation. For camber roofs, the parameter models are selected. The feature parameters are determined in the point cloud fitting procedure. For flat and gable roofs, the interior structure lines need to be determined. We detect image edges within the building polygons. The polygons in the image space are projected by employing the building blocks estimated from the DSM. Hough transform is integrated to select the major structure lines. We then project the structure lines to the object space to generate three dimensional building edges. After a geometric regularization, the building models are generated by employing SMS method. The details are given in Chen et al (2006).

5. EXPERIMENT AND RESULTS

The test data in this experiment include (1) vector maps with 1:1000 scale, (2) digital aerial images with 0.12m resolution, and (3) LIDAR point clouds acquired from Leica ALS50 with a density of 1.5 pts/m². The test area is a part of Hsin-Chu city in north Taiwan. We select four types of building in the validation. As shown in Fig. 3 (a), the first one is the flat roof without miscellaneous goods on the roof. Fig. 3 (b) is the example of the second type of building which is also a flat roof but with tiny and complex annex on the roof. The third one, as shown in Fig. 3 (3), is a gable building. The fourth type is a camber roof, as shown in Fig. 3 (d).

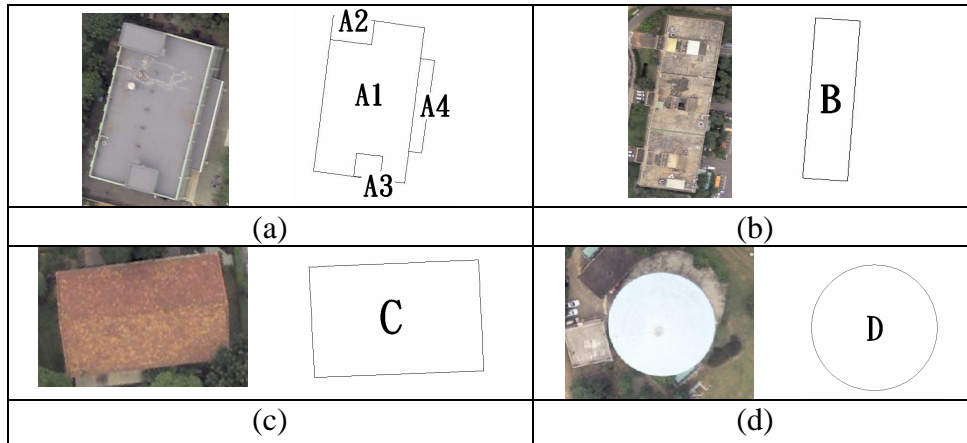


Figure 3 Four building types in the validation

(a) Flat roof, (b) Flat roof with annex structure, (c) Gable roof, (d) Camber roof

Fig. 4 depicts the results of the point cloud filtering for four types of buildings. In each type, the left part is the raw point clouds, while the right one is the results after filtering. It is observed that the unwanted points have been soundly excluded. Tab.1 gives the change of point amounts in the filtering.

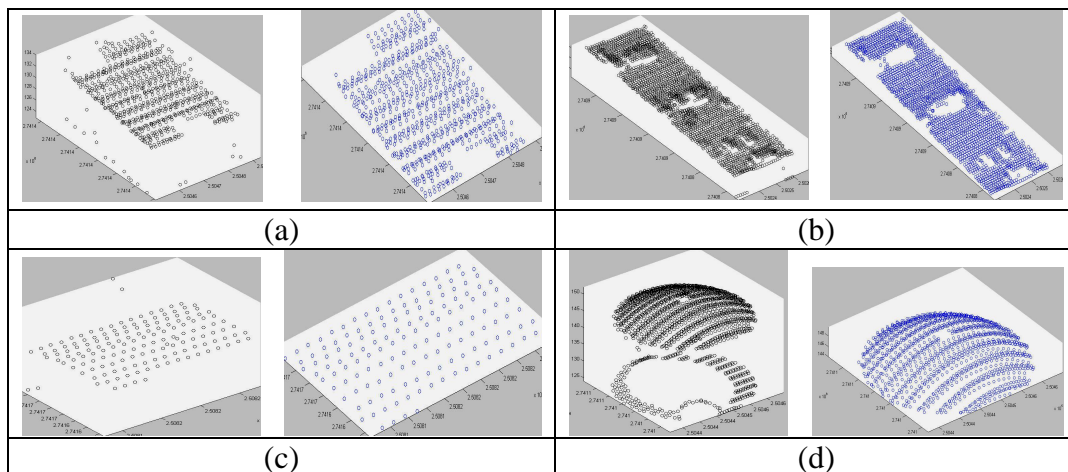


Figure 4 Point clouds filtering

(a) Flat roof, (b) Flat roof with annex structure, (c) Gable roof, (d) Camber roof

Table 1 Number of points in the filtering

Roof type	Roof A1	Roof A2	Roof A3	Roof A4	Roof B	Roof C	Roof D
original points	741	60	41	96	2425	154	1658
filtration points	644	49	27	48	1950	135	1165

For the determination of building types, we test seven polygons. Notice that building A has four parts, namely A1, A2, A3, and A4. As shown in Fig. 3, the remaining three are given as B, C, and D. The fitting procedure is employed to each polygon that is divided into four parts, as indicated in Fig. 2. As shown in Tab.2, the fitting results indicate that parts A1, A2, A3, A4, and B fulfill the condition of flat roof. That means the fitting for a plane is more likely than a sphere. In addition, no significant difference is detected between two orthogonal directions. On the other hand, roof C satisfies the gable building, because two parts in one direction has better fit for a plane than its orthogonal counterparts. The roof D is better fitted as a sphere than a plane by the indication of fitting error. The results reveal the soundness of the proposed method.

Table 2 Result of surface fitting (Unit:meter)

	Roof A1				Roof A2			
Plane	0.090	0.078	0.082	0.086	0.060	0.054	0.072	0.053
Sphere	0.457	1.011	0.885	1.036	0.243	0.292	0.101	0.167
	Roof A3				Roof A4			
Plane	0.070	0.032	0.040	0.073	0.233	0.147	0.055	0.194
Sphere	0.359	0.095	0.077	0.144	0.461	0.976	1.177	0.256
	Roof B				Roof C			
Plane	0.502	0.405	0.542	0.348	0.330	0.310	0.034	0.040
Sphere	8.014	3.189	7.005	3.104	0.197	0.256	0.127	0.273
	Roof D							
Plane	1.333	1.261	1.208	1.221				
Sphere	0.135	0.127	0.134	0.129				

Fig. 5 shows the result of modeling in each roof types. In each type, the right part is building model. As shown in Fig. 5 (a) and Fig. 5 (b), the left parts depict the topology of the building boundaries superimposed with the point clouds from LIDAR. Fig. 5 (c) indicates the ridge be intersection of two adjacent planar faces. And Fig. 5 (d) depicts the camber roof in polyhedral structure. Notice that the model-based parameters have been transformed to the polyhedral ones for the unified presentation with others.

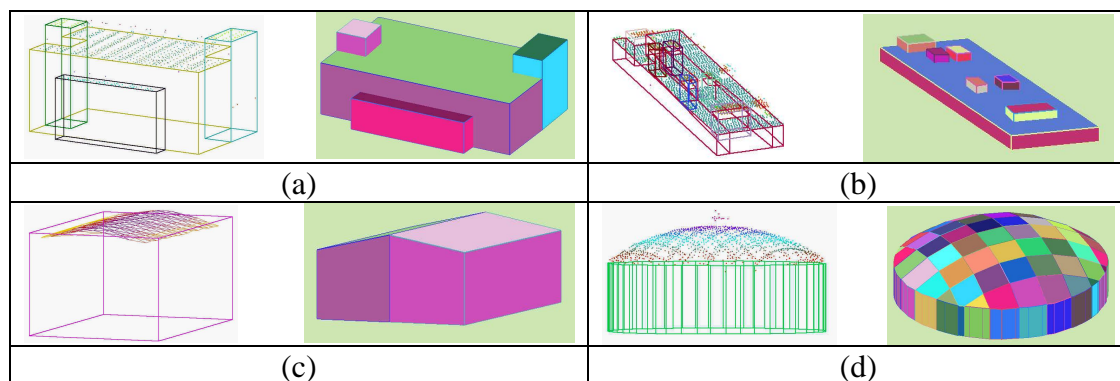


Figure 5 Result of building models

(a) Flat roof, (b) Flat roof with annex structure, (c) Gable roof, (d) Camber roof

6. CONCLUSIONS

We have presented a scheme for the roof classification and building modeling by the fusion of LIDAR data, aerial images and vector maps. The results from the experiment show the potential of the proposed method. Each building type could be classified and reconstructed successfully by the proposed approach.

ACKNOWLEDGEMENT

This investigation was partially supported by the National Science Council of Taiwan under Project NSC 95 - 2221 - E - 008 - 103 - MY2.

REFERENCES

- Canny, J., 1986. A Computational Approach to Edge Detection, IEEE Transactions on Pattern Analysis and Machine Intelligence, Vol 8, No. 6, pp.679-698
- Chen, L.J., Teo, T.A., Hsien, C.H., and Rau, J.Y., 2006. Reconstruction of building models with curvilinear from laser scanner and aerial imagery, Lecture Notes in Computer Science, in press.
- Golias, N. A. and Dutton, R. W., 1997. Delaunay triangulation and 3D adaptive mesh generation, Finite Element in Analysis and Design, Vol. 25, pp. 331-341.
- Habib, F.A., Kim, C. J., Kim, E.M., 2005. Linear Features for semi-Automatic Registration and Change Detection of Multi-Source Imagery, LIDAR,IEEE, International Geoscience & Remote Sensing Symposium, Vol.66, pp.2117-2120.
- Mannan, M.A., Juergen, B., 2004. Virtual Environments in Planning Affairs, IAPRS International Archives of Photogrammetry and Remote Sensing, Vol.35, Part B8, pp.22-26.
- Mortenson, M. E., 1999. Mathematic for computer graphics application, Industrial Press, New York, 2nd edition, pp. 202-204.
- Overby J., Bodum L., Kjems E., Ilsøe P.M., 2004. Automatic 3d Building Reconstruction from Airborne Laser Scanning and Cadastral Data Using Hough Transform, IAPRS International Archives of Photogrammetry and Remote Sensing, Vol. 35, Part B3, pp.298-303.
- Rau, J. Y., Chen, L. C., 2003. Robust Reconstruction of Building Models from Three-Dimensional Line Segments, Photogrammetry Engineering & Remote Sensing, Vol. 69, No .2, pp. 181-188.
- Rottensteiner, F., Briese, C., 2003. Automatic Generation of Building Models from LiDAR Data and the Integration of Aerial Images. IAPRS International Archives of Photogrammetry and Remote Sensing, Vol. 34, Part3/W13, pp.298-303.
- Schwalbe, E., Maas, H. G., Seidel, F., 2005. 3D building model generation from airborne laserscanner data using 2D GIS data and orthogonal point cloud projections, IAPRS International Archives of Photogrammetry and Remote Sensing, Vol.36, Part 3/W19, pp.209-214.
- Suveg, I., Vosselman, G., 2004. Reconstruction of 3D building models from aerial images and maps, ISPRS Journal of Photogrammetry & Remote Sensing, Vol. 58, pp. 202-224.
- Taillandier, F., 2005. Automatic Building Reconstruction from Cadastral Maps and Aerial Images, IAPRS International Archives of Photogrammetry and Remote Sensing, Vol.36, Part 3/W24, pp.105-110.
- Tseng, Y. H., & Wang, S., 2003. Semiautomatic building extraction based on CSG model-image fitting, Photogrammetric Engineering & Remote Sensing, Vol. 69, No. 2, February 2003, pp. 171-179.
- Zhang, Y.J., Zhang, Z.Z., Zhang, J.Q., Wu, J., 2005, 3D building modeling with digital map, LIDAR data and video image sequences, The Photogrammetric Record, Vol.20, pp.285-302.